

This is the accepted manuscript made available via CHORUS. The article has been published as:

## Discovering colorons at the early stage LHC

Duane A. Dicus, Chung Kao, S. Nandi, and Joshua Sayre

Phys. Rev. D **83**, 091702 — Published 18 May 2011

DOI: [10.1103/PhysRevD.83.091702](https://doi.org/10.1103/PhysRevD.83.091702)

# Discovering Colorons at the Early Stage LHC

Duane A. Dicus<sup>a\*</sup>, Chung Kao<sup>b†</sup>, S. Nandi<sup>c‡</sup>, Joshua Sayre<sup>b§</sup>

<sup>a</sup>*Center for Particles and Fields and Texas Cosmology Center, University of Texas, Austin, TX 78712, USA*

<sup>b</sup>*Homer L. Dodge Department of Physics and Astronomy and Oklahoma Center for High Energy Physics,  
University of Oklahoma, Norman, OK 73019, USA*

<sup>c</sup>*Department of Physics and Oklahoma Center for High Energy Physics,  
Oklahoma State University, Stillwater, OK 74078, USA*

(Dated: April 22, 2011)

Prospects are investigated for the discovery of massive hyper-gluons using data from the early runs of the Large Hadron Collider. A center of mass energy of 7 TeV and an integrated luminosity of  $1 \text{ fb}^{-1}$  or  $5 \text{ fb}^{-1}$  are assumed. A phenomenological Lagrangian is adopted to evaluate the cross section of a pair of colored vector bosons (colorons,  $\tilde{\rho}$ ) decaying into four colored scalar resonances (hyper-pions,  $\tilde{\pi}$ ), which then decay into eight gluons. The dominant eight-jet background from the production of  $8g$ ,  $7g1q$ ,  $6g2q$ , and  $5g3q$  is included. We find an abundance of signal events and that realistic cuts reduce the background enough to establish a  $5\sigma$  signal for the coloron mass of up to 733 GeV with  $1 \text{ fb}^{-1}$  or 833 GeV with  $5 \text{ fb}^{-1}$ .

*Introduction.*— With the LHC collecting data at a center of mass energy of 7 TeV, and with the promise of an accumulation of 1 to  $5 \text{ fb}^{-1}$  of luminosity at this energy, it is sensible to ask what can be learned from this data beyond looking for the Higgs or signs of supersymmetry. Some scenarios have been proposed where the new physics manifests itself solely through the strong force. In particular, if new colored particles exist at TeV scales, they will be discovered through decays into jets. One such possibility is a massive vector boson in the color-octet representation [1–3]. Such a particle has been dubbed a coloron. According to this definition, several theories of physics beyond the Standard Model (SM) give rise to colorons. Examples are topcolor models [1] and Kaluza-Klein excitations of the gluon in the universal extra-dimensional models [4, 5]. In Ref. [6], Kilic, Sundrum and Okui showed how a coloron, as well as a scalar octet, can emerge as the low energy states of an effective theory which arises from a simple model of new, strongly interacting fermions, charged under a new strong interaction as well as QCD color. In this paper we consider that model, following the analysis of Ref. [6] and the subsequent treatment found in Ref. [7].

Briefly the model supposes there exists a new strong force (hypercolor) which becomes confining at a higher energy than the strong QCD force. Fermions (hyperquarks) which carry hypercolor will form bound states which are hypercolor singlets but carry QCD color quantum numbers. The hyperquarks are electroweak singlets so they are allowed by electroweak precision constraints.

In addition, these hyperquarks are triplets of QCD and their lightest bound states are color octets. These recall the  $\rho$  meson flavor octet of ordinary QCD, but are hypercolor singlets in a color octet. These hyper-gluons are the colorons. Analogous to the breaking of chiral symmetry in the Standard Model, this model will also produce, in a color-octet representation, relatively light scalars (hyper-pions) as pseudo-Goldstone bosons.

These vector and scalar octets have an interesting phenomenology. Naively one might think that light octets are severely constrained by dijet searches at the Tevatron [8]. However, in this model the hyper-pions couple sufficiently weakly to gluons to leave unrestricted an interesting parameter range, and the colorons have only a small branching fraction to decay into two quarks or two gluons. Rather, the colorons decay predominantly to hyper-pions, each of which then decays to a gluon pair. Thus the dominant signal for resonant production of a coloron is a 4-jet decay chain. The hyper-pions are the lightest bound state formed by hyperquarks. We assume the branching ratio  $B(\tilde{\pi} \rightarrow gg)$  to be one, similar to  $B(\pi^0 \rightarrow \gamma\gamma)$ , since all other decay channels are greatly suppressed.

On the other hand, there are several processes which pair produce hyper-pions without a resonant coloron. Combined with the loss of jet resolution during showering, hadronization, and reconstruction, this may make the initial coloron resonance difficult to establish. Instead we consider the pair production of colorons, leading to an eight-jet signal and use this signal as a potential discovery mechanism. The LHC is currently running at a center of mass energy of 7 TeV; we present results for possible detection at this energy for two cases of the integrated luminosity,  $1 \text{ fb}^{-1}$  or  $5 \text{ fb}^{-1}$ .

*A Model with Colored Vector Bosons and Scalars.*— The effective Lagrangian for the massive color octets can

---

\*Email address: dicus@physics.utexas.edu

†Email address: kao@physics.ou.edu

‡Email address: s.nandi@okstate.edu

§Email address: sayre@physics.ou.edu

be derived by analogy with the spontaneous breaking of chiral symmetry in the Standard Model. The interactions of the hyper-pions ( $\tilde{\pi}$ ) and the colorons ( $\tilde{\rho}$ ) are given by [7]:

$$\begin{aligned} \mathcal{L}_{\text{eff}} = & -\frac{1}{4}G_{\mu\nu}^a G^{a\mu\nu} + \bar{q}i\not{D}q - \frac{1}{4}\tilde{\rho}_{\mu\nu}^a \tilde{\rho}^{a\mu\nu} + \frac{M_{\tilde{\rho}}^2}{2}\tilde{\rho}_{\mu}^a \tilde{\rho}^{a\mu} \\ & - g_3 \epsilon \tilde{\rho}_{\mu}^a \bar{q} \gamma^{\mu} T^a q + \frac{1}{2}(D_{\mu}\tilde{\pi})^a (D^{\mu}\tilde{\pi})^a - M_{\tilde{\pi}}^2 \tilde{\pi}^a \tilde{\pi}^a \\ & - i g_{\tilde{\rho}\tilde{\pi}\tilde{\pi}} f^{abc} \tilde{\rho}^{a\mu} (\tilde{\pi}^b D_{\mu}\tilde{\pi}^c) - \frac{3g_3^2 \epsilon^{\mu\nu\rho\sigma}}{16\pi^2 f_{\tilde{\pi}}} \text{Tr}[\tilde{\pi} G_{\mu\nu} G_{\rho\sigma}] \\ & + i\chi g_3 \text{Tr}[G_{\mu\nu}[\tilde{\rho}^{\mu}, \tilde{\rho}^{\nu}]]. \end{aligned} \quad (1)$$

The number of hypercolors has been set to be  $N_{\text{HC}} = 3$  for simplicity.  $G_{\mu\nu}$  and  $q$  are SM gluon and quark fields, while  $a$  is a color index.  $D_{\mu}$  is the SM covariant derivative and  $g_3$  the coupling constant of QCD.  $T^a$  and  $f^{abc}$  are, respectively, the generators and structure constants of  $SU(3)$ . Kilic et al. have derived the remaining constants, by analogy with the phenomenology of SM mesons, in terms of  $M_{\tilde{\rho}}$ . They set the  $\tilde{\rho}$ -quark coupling  $\epsilon \simeq 0.2$ , the strongly induced  $\tilde{\rho}-\tilde{\pi}-\tilde{\pi}$  coupling  $g_{\tilde{\rho}\tilde{\pi}\tilde{\pi}} \simeq 6$ , the  $\tilde{\pi}$  decay constant  $f_{\tilde{\pi}} \simeq f_{\pi} \times \frac{M_{\tilde{\rho}}}{M_{\rho}}$ , where  $f_{\pi}$  and  $M_{\rho}$  are the ordinary pion decay constant (92 MeV) and  $\rho$  mass, and the mass relation  $M_{\tilde{\pi}} \simeq 0.3 \times M_{\tilde{\rho}}$ . Thus a value of  $M_{\tilde{\pi}}$  determines the value of  $M_{\tilde{\rho}}$ . Note that the last term of the Lagrangian contains a free parameter  $\chi$  which cannot be extrapolated from the Standard Model.

*Production Cross Section.*— We have evaluated the cross section for  $pp \rightarrow \tilde{\rho}\tilde{\rho} \rightarrow 4\tilde{\pi} \rightarrow 8g + X$  from gluon fusion and quark-antiquark fusion in two ways, (a) with a complete matrix element involving Breit-Wigner resonances for both  $\tilde{\rho}$  and  $\tilde{\pi}$ , and (b) with matrix elements involving Breit-Wigner resonances for the  $\tilde{\rho}$  in  $pp \rightarrow \tilde{\rho}\tilde{\rho} \rightarrow 4\tilde{\pi} + X$  and the narrow width approximation for  $\tilde{\pi} \rightarrow gg$ . We calculate the decay widths as  $\Gamma_{\tilde{\rho}} \simeq 0.19 \times M_{\tilde{\rho}}$ , and  $\Gamma_{\tilde{\pi}} \simeq 0.12\alpha_s^2 \times M_{\tilde{\pi}}$ . Thus, the  $\tilde{\pi}$  width is narrow and, in the narrow width approximation, the cross section for  $pp \rightarrow \tilde{\rho}\tilde{\rho} \rightarrow 4\tilde{\pi} \rightarrow 8g + X$  can be thought of as the production cross section  $\sigma(pp \rightarrow \tilde{\rho}\tilde{\rho} \rightarrow 4\tilde{\pi} + X)$  multiplied by the branching fraction of hyper-pions decay into gluon pairs  $B(\tilde{\pi} \rightarrow gg) = 1$ . In addition, we have checked  $|M|^2(gg \rightarrow \tilde{\rho}\tilde{\rho} \rightarrow 4\tilde{\pi})$  analytically. We have added the model of Eq.(1) to MadGraph [10, 11] to generate the matrix element squared for the processes (a) and (b). The numerical output from MadGraph gives excellent agreement with that from our analytic expressions.

With energy-momentum smearing, the cross section in the narrow width approximation agrees very well with that evaluated with Breit-Wigner resonances for the hyper-pion. The ATLAS detector specifications [12] have been adopted to Gaussian smear the momenta of the jets by  $\frac{\Delta E}{E} = \frac{0.60}{\sqrt{E(\text{GeV})}} \oplus 0.03$ , with individual terms added in quadrature.

We use the parton distribution functions of CTEQ6L1

[9]. The factorization scale as well as the renormalization scale is chosen to be (a) the coloron mass ( $M_{\tilde{\rho}}$ ) for the coloron signal, and (b) the root mean square transverse momentum ( $\sqrt{\langle p_T^2 \rangle}$ ) of all eight jets for the background, with leading order evolution of the strong coupling. For simplicity, the  $K$  factor is taken to be one for both the signal and the background.

To demonstrate that colorons can be produced copiously at the early LHC, we derived an analytic expression for the square of the matrix element, summed over polarizations, for  $gg \rightarrow \tilde{\rho}\tilde{\rho}$ . In Fig. 1 we show the cross section for  $pp \rightarrow \tilde{\rho}\tilde{\rho} + X$  for a few values of  $\chi$ . For this figure we did not make any cuts. The theory is only unitary for  $\chi = 1$  where the terms in the square of the matrix element which grow with energy are absent; in the remainder of the paper that is the only value we will use. For  $\chi = 1$  we have checked that our results for  $gg \rightarrow \tilde{\rho}\tilde{\rho}$  are consistent with those of Refs. [2, 3, 7] for  $\sqrt{s} = 14$  TeV.

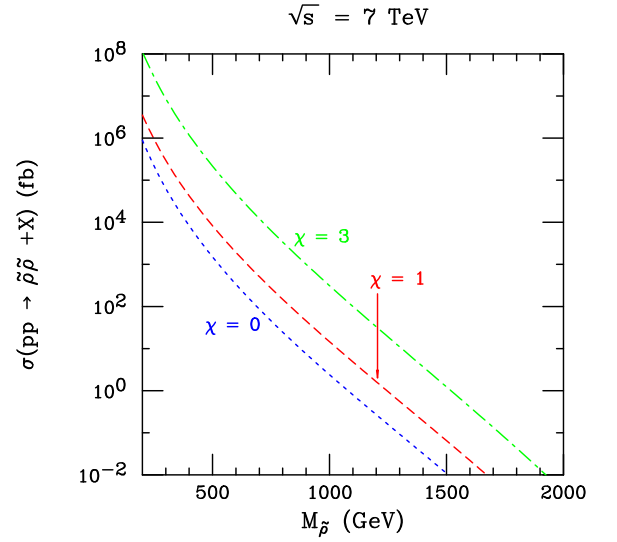


FIG. 1: The cross section of  $pp \rightarrow \tilde{\rho}\tilde{\rho} + X$  as a function of  $M_{\tilde{\rho}}$  for  $\chi = 1, 0$ , and  $3$ .

*Physics Background.*— We compute the cross section of the dominant eight jet physics background with the matrix-element generator COMIX [13], interfaced with the event generator SHERPA [14]. COMIX adopts color-dressed Berends-Giele recursion relations [15, 16] to construct QCD amplitudes. The backgrounds included are, in the order of importance,  $gq \rightarrow 7g1q$ ,  $gg \rightarrow 8g$ ,  $gq \rightarrow 5g3q$ ,  $qq \rightarrow 6g2q$ , and  $gg \rightarrow 6g2q$ , where  $q$  may be a quark or anti-quark). For  $M_{\tilde{\pi}} \gtrsim 230$  GeV, the  $6g2q$  process becomes larger than the  $8g$  process. These dominant processes involve the largest number of diagrams and biggest color factors, with initial valence quarks becoming important at higher energies.

To reduce the large QCD physics background, we require that in each event, signal or background, there

should be eight jets ( $j = g, q, \bar{q}$ ) with lower limits on their transverse momenta of  $p_T(j_1, \dots, j_8) \geq 250, 200, 160, 120, 80, 60, 40, 20$  GeV, a pseudo-rapidity for each jet of  $|\eta(j)| < 2.5$ , and angular separation for each pair of jets of  $\Delta R = \sqrt{\Delta\phi^2 + \Delta\eta^2} > 0.5$ . A hierarchical set of  $p_T$  cuts is chosen because the leading jet has a broad peak near  $M_{\tilde{\rho}}/2$  in the  $p_T$  distribution for  $\tilde{\rho}\tilde{\rho} \rightarrow 4\tilde{\pi} \rightarrow 8g$ , which is from the Jacobian peak of  $\tilde{\rho} \rightarrow \tilde{\pi}\tilde{\pi}$ , while the 8th jet typically peaks around 40 GeV.

*Discovery Potential at the Early LHC.*— To study the discovery potential of  $pp \rightarrow \tilde{\rho}\tilde{\rho} \rightarrow 4\tilde{\pi} \rightarrow 8g + X$ , we evaluate the cross sections for the signal and background as described in the previous section with, in addition, two types of mass cuts: (i) *relative* mass cuts and (ii) *fixed* mass cuts.

The *relative* mass cut requires that within each event the eight jets can be arranged into four pairs of jets that have invariant mass within  $\Delta M_{2j}$  of each other, and there must be distinct pairs of four jets that have invariant mass within  $\Delta M_{4j}$  of each other. We have chosen (a)  $\Delta M_{2j} \leq 30$  GeV and  $\Delta M_{4j} \leq 60$  GeV or (b)  $\Delta M_{2j} \leq 50$  GeV and  $\Delta M_{4j} \leq 100$  GeV.

The *fixed* mass cut requires that within each event, there must be eight jets with four pairs of jets that have invariant mass within a bin of width  $\pm\Delta M_{2j}$  centered at  $M_{\tilde{\pi}}$ , and there must be two groups of four jets that have invariant mass within a bin of width  $\pm\Delta M_{4j}$  centered at  $M_{\tilde{\rho}}$ . We have chosen (a)  $|M_{2j} - M_{\tilde{\pi}}| \leq 0.10M_{\tilde{\pi}}$  and  $|M_{4j} - M_{\tilde{\rho}}| \leq 0.15M_{\tilde{\rho}}$  or (b)  $|M_{2j} - M_{\tilde{\pi}}| \leq 0.15M_{\tilde{\pi}}$  and  $|M_{4j} - M_{\tilde{\rho}}| \leq 0.20M_{\tilde{\rho}}$ . Our choice of mass window is consistent with the CMS [17] and the ATLAS [18] dijet mass resolution, which is between 16% to 10% for masses from 0.5 TeV to 2.5 TeV. This fixed mass cut has more power to discriminate against the background. However, in practice  $M_{\tilde{\rho}}$  and  $M_{\tilde{\pi}}$  are unknown and candidate masses must be scanned over to determine mass peaks, which makes it harder to implement.

We define the signal to be observable if the lower limit on the signal plus background is larger than the corresponding upper limit on the background [19] which corresponds to

$$\sigma_s > \frac{N}{L} \left[ N + 2\sqrt{L\sigma_b} \right]. \quad (2)$$

Here  $L$  is the integrated luminosity, assumed to be  $1 \text{ fb}^{-1}$  or  $5 \text{ fb}^{-1}$ ,  $\sigma_s$  is the value of the cross section that the signal cross section must exceed, and  $\sigma_b$  is the background cross section. The parameter  $N$  specifies the level or probability of discovery. We take  $N = 2.5$ , which corresponds to a  $5\sigma$  threshold in the limit  $\sigma_s \ll \sigma_b$ , a condition that will be true for the relative mass cuts. If the background has fewer than 16 events, assuming  $1 \text{ fb}^{-1}$  of luminosity, as will often be the case for the fixed mass cuts, we employ a Poisson distribution and require that the Poisson probability for the SM background to fluctuate to this level is less than  $2.85 \times 10^{-7}$ .

To assess the discovery potential we present in Fig. 2 the cross sections of the coloron signal, and the eight jet background, after acceptance cuts and *relative* mass cuts, versus  $M_{\tilde{\pi}}$ . In addition, we present the minimal signal cross section that is required to establish a  $5\sigma$  effect.

Fig. 2 shows that the narrower relative mass cut (a) has the potential to discover the hyper-pions and colorons up to  $M_{\tilde{\pi}} = 195$  GeV ( $M_{\tilde{\rho}} = 650$  GeV) for  $1 \text{ fb}^{-1}$ . The wider relative mass cut (b) will allow more background events, and thus has a slightly reduced discovery reach of  $M_{\tilde{\pi}} = 185$  GeV ( $M_{\tilde{\rho}} = 617$  GeV). Fig. 2 shows the 5 sigma limit for  $1 \text{ fb}^{-1}$  only. The 5 sigma limit for  $5 \text{ fb}^{-1}$  is  $M_{\tilde{\pi}} = 220$  GeV ( $M_{\tilde{\rho}} = 733$  GeV for cuts (a) or  $M_{\tilde{\pi}} = 210$  GeV ( $M_{\tilde{\rho}} = 700$  GeV) for cuts (b). Thus using Eq.(2) does not show much difference between the results with cuts (a) or (b). However, if instead of (2) we use the signal to background ratio as a measure of merit, we see that the relative mass cut (a) is significantly better.

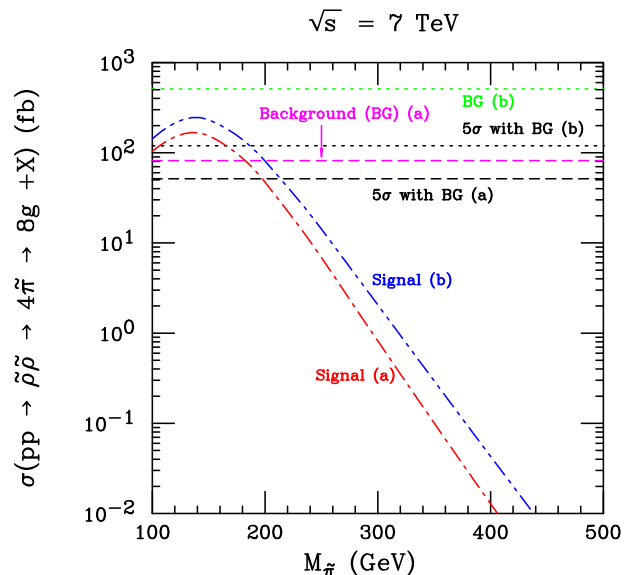


FIG. 2: The cross section for  $pp \rightarrow \tilde{\rho}\tilde{\rho} \rightarrow 4\tilde{\pi} \rightarrow 8g + X$  as a function of  $M_{\tilde{\pi}}$ . We have applied kinematic cuts on  $p_T$ ,  $\eta$ ,  $\Delta R$  and two sets of relative mass cuts: (a)  $\Delta M_{2j} < 30$  GeV and  $\Delta M_{4j} < 60$  GeV [red, dot-dash], or (b)  $\Delta M_{2j} < 50$  GeV and  $\Delta M_{4j} < 100$  GeV [blue, dot-dotted]. Also shown are the background cross section for the SM processes from the production of  $8g$ ,  $7g1q$ ,  $6g2q$ , and  $5g3q$  with relative mass cut (a) [magenta, dash] and relative mass cut (b) [green, dot]. In addition, we present the minimal signal cross section that is required by a 5 sigma criterion with relative mass cut (a) [dash] and relative mass cut (b) [dot] assuming an integrated luminosity of  $1 \text{ fb}^{-1}$ .

Figure 3 shows cross sections of the coloron signal and the background from the production of  $8g$ ,  $7g1q$ ,  $6g2q$ , and  $5g3q$ , with acceptance cuts and *fixed* mass cuts versus  $M_{\tilde{\pi}}$ . We have replaced the relative mass cuts of Fig. 2 with the two sets of fixed mass cuts given above. Also shown is the minimal signal cross

section that is required by the 5 sigma criterion. For  $M_{\tilde{\pi}} = 100$  GeV it is very time consuming to get a convergent cross section for the background. So to improve the stability we have applied somewhat less stringent  $p_T$  cuts than those given in above,  $p_T(j_1, \dots, j_8) \geq 200, 150, 120, 100, 80, 60, 40, 20$  GeV respectively. Therefore, the background cross section (red, cross) and the corresponding 5 $\sigma$  signal cross section (green, diamond) for  $M_{\tilde{\pi}} = 100$  GeV are presented with symbols. We note that even with lower  $p_T$  cuts, the background is negligible. Using Eq. (2) we see that the narrower fixed mass cut (a), has the potential to discover the hyper-pions and colorons up to  $M_{\tilde{\pi}} = 220$  GeV ( $M_{\tilde{\rho}} = 733$  GeV) for 1 fb $^{-1}$  of luminosity or  $M_{\tilde{\pi}} = 250$  GeV ( $M_{\tilde{\rho}} = 833$  GeV) for 5 fb $^{-1}$ . The wider fixed mass cut (b) will allow more background events, which results in a slightly reduced discovery reach of  $M_{\tilde{\pi}} = 210$  GeV ( $M_{\tilde{\rho}} = 700$  GeV) (1 fb $^{-1}$ ) or  $M_{\tilde{\pi}} = 235$  GeV ( $M_{\tilde{\rho}} = 783$  GeV) (5 fb $^{-1}$ ). Again the different sets of cuts do not give a significantly different reach in  $M_{\tilde{\pi}}$  as calculated from (2) but they do give a significantly different ratio of signal to background.

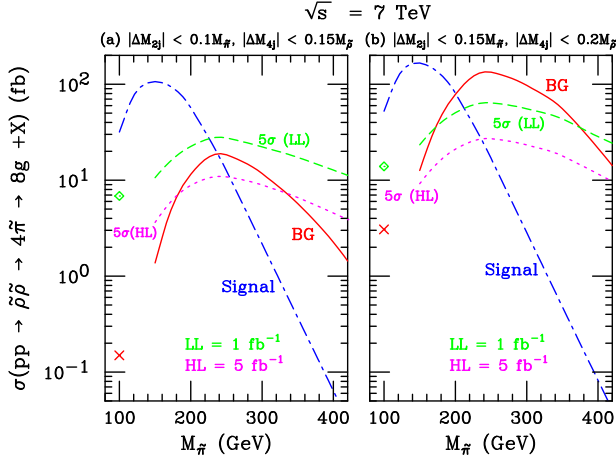


FIG. 3: The cross section for  $pp \rightarrow \tilde{\rho}\tilde{\rho} \rightarrow 4\tilde{\pi} \rightarrow 8g + X$  (blue, dot-dash) as a function of  $M_{\tilde{\pi}}$  with acceptance cuts on  $p_T$ ,  $\eta$ , and  $\Delta R$  and the two sets of fixed mass cuts shown on the top axis. Also shown are the SM background cross section (BG) (red, solid) with the same cuts and the minimal signal cross section that is required by the 5 sigma criterion (green, dash) or (red, dash). For  $M_{\tilde{\pi}} = 100$  GeV, the 5 $\sigma$  signal cross section and background (green diamond, red cross) are calculated with lower  $p_T$  cuts.

*Conclusions.*— We have demonstrated that colorons and hyper-pions can be produced abundantly at the early stage of the LHC with a center of mass energy  $\sqrt{s} = 7$  TeV and an integrated luminosity of 1 fb $^{-1}$  or 5 fb $^{-1}$ . We give two types of mass cuts which, when used in addition to standard acceptance cuts, reduce the background sufficiently to establish a 5 $\sigma$  signal as large as  $M_{\tilde{\pi}} \lesssim 220$  GeV ( $M_{\tilde{\rho}} \lesssim 733$  GeV) for 1 fb $^{-1}$  or  $M_{\tilde{\pi}} \lesssim 250$  GeV ( $M_{\tilde{\rho}} \lesssim 833$  GeV) for 5 fb $^{-1}$ .

Naturally, our estimates are subject to higher-order corrections which may be substantial in the case of the background. However Fig. 3 shows that a factor of two increase in the background would only degrade our discovery limit by  $\sim 20$  GeV. In the same spirit we used definite relations between the parameters (as listed below Eq.(1)) but reasonable changes in these relations will not have much effect on our results as long as the hyper-pion width remains narrow.

*Acknowledgments.*— This research was supported in part by the U.S. Department of Energy under Grants No. DE-FG02-04ER41305, No. DE-FG03-93ER40757, No. DE-FG02-04ER41306 and No. DE-FG02-04ER46140.

- 
- [1] C. T. Hill, Phys. Lett. B **266**, 419 (1991).
  - [2] D. A. Dicus, B. Dutta and S. Nandi, Phys. Rev. D **51**, 6085 (1995) [arXiv:hep-ph/9412370].
  - [3] B. A. Dobrescu, K. Kong and R. Mahbubani, Phys. Lett. B **670**, 119 (2008) [arXiv:0709.2378 [hep-ph]].
  - [4] T. Appelquist, H. C. Cheng and B. A. Dobrescu, Phys. Rev. D **64**, 035002 (2001) [arXiv:hep-ph/0012100].
  - [5] D. A. Dicus, C. D. McMullen and S. Nandi, Phys. Rev. D **65**, 076007 (2002) [arXiv:hep-ph/0012259].
  - [6] C. Kilic, T. Okui and R. Sundrum, JHEP **0807**, 038 (2008) [arXiv:0802.2568 [hep-ph]].
  - [7] C. Kilic, S. Schumann and M. Son, JHEP **0904**, 128 (2009) [arXiv:0810.5542 [hep-ph]].
  - [8] T. Aaltonen *et al.* [CDF Collaboration], Phys. Rev. D **79**, 112002 (2009) [arXiv:0812.4036 [hep-ex]].
  - [9] J. Pumplin, D. R. Stump, J. Huston, H. L. Lai, P. Nadolsky and W. K. Tung, JHEP **0207**, 012 (2002), [arXiv:hep-ph/0201195].
  - [10] T. Stelzer and W. F. Long, Nucl. Phys. Proc. Suppl. **37B** (1994) 158.
  - [11] H. Murayama, I. Watanabe and K. Hagiwara, “HELAS: HELicity amplitude subroutines for Feynman diagram evaluations,” KEK report KEK-91-11 (1992).
  - [12] ATLAS Collaboration, ATLAS Detector and Physics Performance Technical Design Report, CERN/LHCC 99-14/15 (1999); G. Aad *et al.* [The ATLAS Collaboration], arXiv:0901.0512 [hep-ex].
  - [13] T. Gleisberg and S. Hoeche, JHEP **0812**, 039 (2008) [arXiv:0808.3674 [hep-ph]].
  - [14] T. Gleisberg, S. Hoeche, F. Krauss, A. Schalicke, S. Schumann and J. C. Winter, JHEP **0402**, 056 (2004) [arXiv:hep-ph/0311263].
  - [15] F. A. Berends and W. T. Giele, Nucl. Phys. B **306**, 759 (1988).
  - [16] C. Duhr, S. Hoeche and F. Maltoni, JHEP **0608**, 062 (2006) [arXiv:hep-ph/0607057].
  - [17] V. Khachatryan *et al.* [CMS Collaboration], Phys. Rev. Lett. **105**, 211801 (2010) [arXiv:1010.0203 [hep-ex]].
  - [18] G. Aad *et al.* [ATLAS Collaboration], arXiv:1103.3864 [hep-ex].
  - [19] H. Baer, M. Bisset, C. Kao and X. Tata, Phys. Rev. D **46**, 1067 (1992).